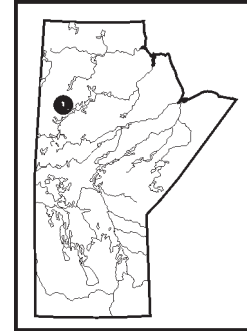


**GS-9      Rock and spruce-bark analyses in the vicinity of a zone of  
‘barren sulphide’: implications for exploration of the  
Sheila-Margaret lakes area, Lynn Lake, Manitoba (NTS 64C14)  
by G.H. Gale**



Gale, G.H. 2004: Rock and spruce-bark analyses in the vicinity of a zone of ‘barren sulphide’: implications for exploration of the Sheila-Margaret lakes area, Lynn Lake, Manitoba (NTS 64C14); *in* Report of Activities 2004, Manitoba Industry, Economic Development and Mines, Manitoba Geological Survey, p. 104–114.

### Summary

Whole-rock analyses from some sulphide-bearing rocks in a zone of ‘barren sulphide’ at Sheila Lake contain anomalous concentrations of base and precious metals. Rare earth element (REE) analyses of associated sulphide-rich layers and hostrocks show positive europium deviation ( $\text{Eu}^d$ )<sup>1</sup> values. The sulphide-bearing rocks are interpreted to represent distal exhalites to a volcanogenic hydrothermal vent that was capable of producing a mineral deposit. Ashed spruce bark from the mineralized zone is anomalous in the same metals as those detected in the underlying rocks. The REE element enhancement in bark ash from the mineralized zone is due to a secondary process such as ionic transport in an electrochemical cell. The positive  $\text{Eu}^d$  present in the hostrock analyses is not reflected in the bark ash analyses.

### Introduction

An occurrence of sulphides on the south shore of Sheila Lake consists of several layers of pyritic sedimentary rocks, a solid sulphide layer and chert with trace amounts of Cu, Zn, Pb, Ag and Au; this was described as location 10 by Baldwin (1989) and is referred to here as occurrence 10. This mineral occurrence is hosted by interlayered mafic, intermediate and felsic sedimentary rocks. These rocks are dominantly volcanic derived and appear to represent redeposited pyroclastic rocks. Greywacke is the most common rock observed, although heterolithic volcanic breccia, conglomerate, siltstone and minor mudstone are also present (Baldwin, 1989).

The hostrocks to this mineral occurrence are part of an extensive unit of sedimentary rocks that extends through Sheila and Margaret lakes (Figure GS-9-1). Geophysical surveys indicate the presence of a number of magnetic highs and several electromagnetic conductors within this sequence of sedimentary rocks. Several holes were drilled to test different geophysical anomalies in the mid-1980s (P. Pawliw, pers. comm., 2003).

Rock samples were collected from the mineralization and hostrocks exposed at occurrence 10. In addition, spruce bark was collected across the mineralized zone (Figure GS-9-2). The objectives of this project are to determine 1) if the rare earth element contents can be used as an exploration tool to vector to mineralization; and 2) if the rare earth signatures present in the mineralization can be detected in the bark of spruce trees growing on the occurrence.

This paper presents the results for rock and bark samples collected in 2003. During the current field season, a number of drillcores from the sedimentary sequence were logged.

### Rock geochemistry

Fifteen samples of hostrocks and mineralized material were analyzed for major and trace elements using the 4-Litho standard method at Activation Laboratories, Ancaster, Ontario. Selected data are presented in Table GS-9-1, and the complete analytical dataset is available in Data Repository item 2004005.<sup>2</sup>

The hostrocks to the sulphide mineralization are predominantly mafic to intermediate sedimentary rocks (Baldwin, 1988); several thin beds of light-coloured ‘felsic’ rocks with sulphides are exposed in the trenches. A plot of  $\text{TiO}_2$  versus Zr shows that all of these rocks have  $\text{Zr}/\text{TiO}_2$  ratios similar to those of basalt and andesite (Gale and Dabek, 1996). On Figure GS-9-3, only the rhyolite standard (sample 16) and sample 7 (i.e., 42-10-7), a chert with quartz veins, plot in the field normally occupied by felsic volcanic rocks. The intermediate to mafic provenance of these rocks is confirmed by their position on Figure GS-9-4, where the rhyolite standard also plots well away from the cluster of mafic to intermediate sedimentary rocks.

<sup>1</sup>  $\text{Eu}^d = (\text{Eu}_n / (\text{Sm}_n/2 + \text{Gd}_n/2) - 1) \times 100$ , where  $_n$  is the chondrite-normalized value

<sup>2</sup> MGS Data Repository item 2004005, containing the data or other information sources used to compile this report, is available on-line to download free of charge at [www2.gov.mb.ca/itm-cat/freedownloads.htm](http://www2.gov.mb.ca/itm-cat/freedownloads.htm), or on request from [minesinfo@gov.mb.ca](mailto:minesinfo@gov.mb.ca) or Mineral Resources Library, Manitoba Industry, Economic Development and Mines, 360–1395 Ellice Avenue, Winnipeg, MB R3G 3P2, Canada.

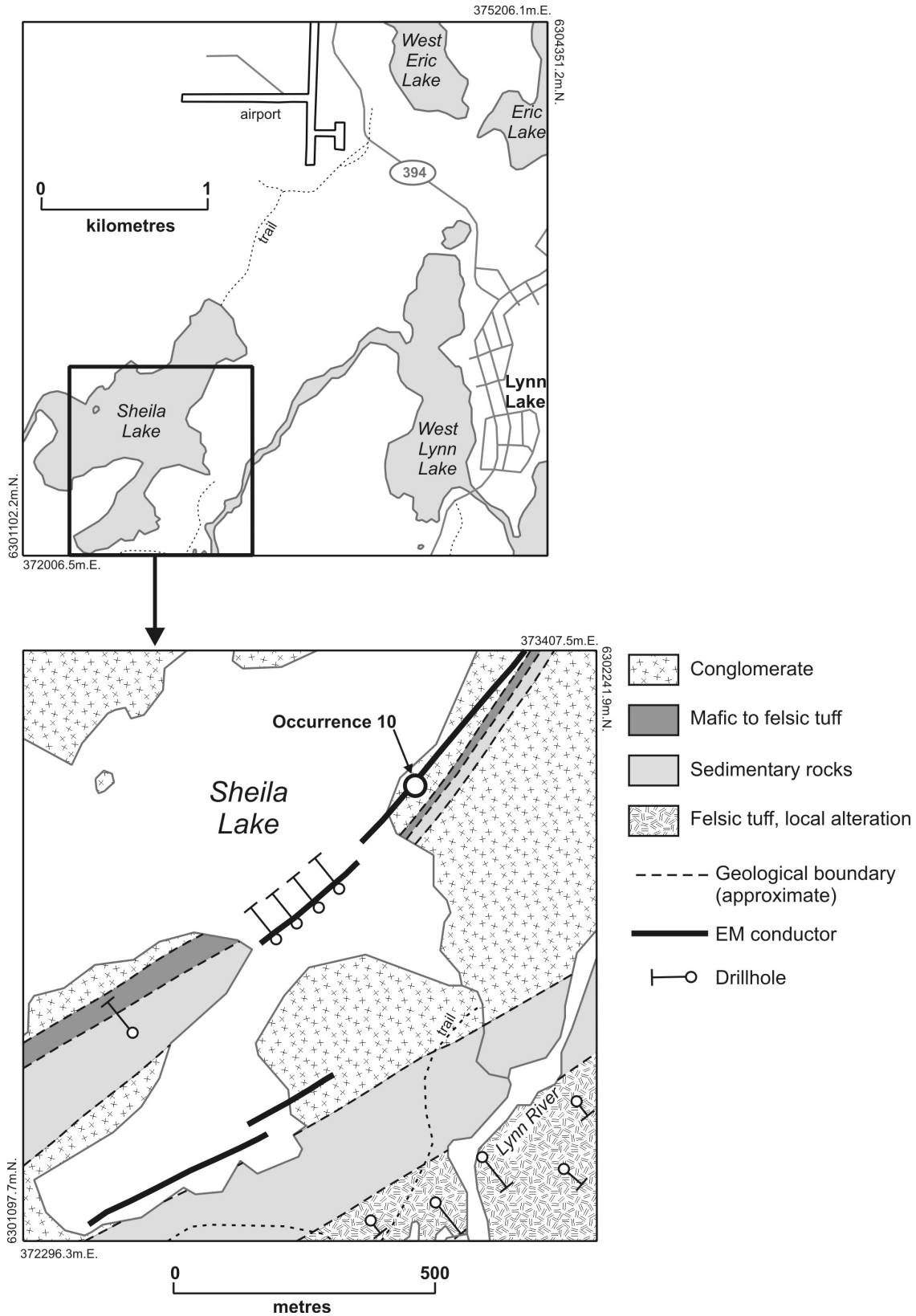


**Figure GS-9-1:** General geology of the Sheila-Margaret lakes area, showing locations of mineral occurrences. Geology provided by Black Hawk Mining Ltd., 2004; index map from Baldwin (1988).

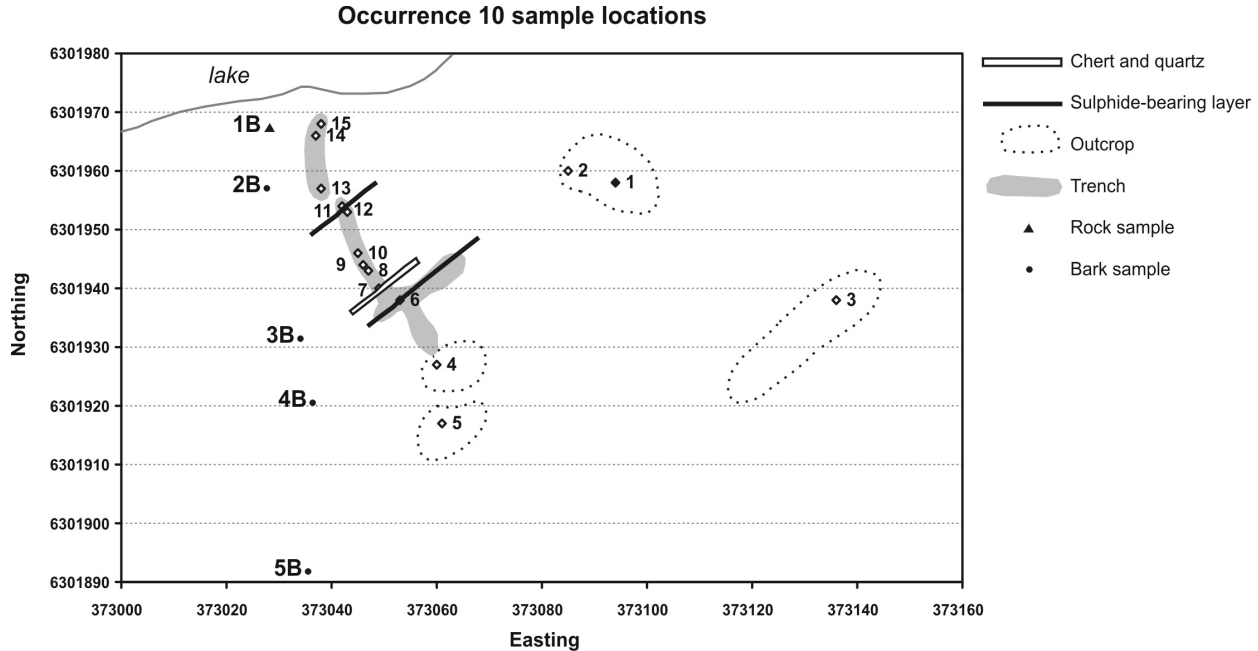


Figure GS-9-2: Location of rock and bark samples at occurrence 10, south shore of Sheila Lake.

Several of the sericitic and sulphidic rocks visually appear to be altered, but all of the samples plot close to the feldspar model line (with slope  $[m] = 1$ ) on Figure GS-9-5a and have therefore undergone little alkali metasomatism. A number of samples (samples 4, 12, 9, 2 and 8) plot well to the right of the main cluster of samples on this diagram; these are the samples that plot in the field normally occupied by basalt on Figure GS-9-3. This suggests that their composition has been modified. Mafic and intermediate volcanic rocks normally plot above the feldspar model line (Madeisky, 1995). The chert sample (sample 7) has low Al and plots closer to the origin than any of the other samples.

If Ca is removed from the equation (Figure GS-9-5b) for the alkali plot and the data are modelled on a Ca-free basis to account for Ca metasomatism, then only samples 7 and 16 plot near the feldspar model line ( $m = 1$ ) and all other samples from the trenches now plot close to or on the sericite line ( $m = 1/3$ ). The hostrock samples 3 and 5, collected well away from the mineralized zone, plot farther from the sericite line than the other hostrock samples (samples 1, 2 and 4). This suggests that little, if any, Ca metasomatism has taken place and that Na and/or K metasomatism can explain why these rocks plot away from the feldspar model line on Figure GS-9-5a. Potassium metasomatism is confirmed by Figure GS-9-6, where the molar plot shows that many of the samples, including the hostrocks, are enriched in K relative to Na and Ca; unaltered samples on this diagram will plot along the feldspar model line, and K-altered samples plot toward the K line ( $m = 1$ ; Madeisky, 1995). Figures GS-9-7a and b are used to discriminate silicified from unaltered rocks; these show that only sample 7, a chert with quartz veins, and sample 11, a weathered sulphide block from the trench with 50% pyrrhotite (and pyrite?), plot away from the trend defined by the hostrocks. Consequently only K metasomatism is recognized in the hostrocks.

The alkali element and Si molar-ratio plots (Figures GS-9-4 to -7) indicate that only minor K metasomatism has affected the hostrocks and the sulphidic mineralization. They also suggest that variations in composition are a result of source material rather than alteration.

Rare earth element data can be used to determine both the provenance of altered and reworked rocks and proximity to a hydrothermal exhalative vent (Gale et al., 1997). In particular, chondrite-normalized europium deviation ( $Eu^d$ ) values show a progressive decrease away from known volcanogenic massive sulphides (Gale et al., 1999; Gale, 2003).

The REE for hostrocks south of occurrence 10 are plotted on Figure GS-9-8a. These show a nearly flat heavy rare earth element (HREE) pattern and light rare earth element (LREE) fractionation, and samples 2, 3 and 4 have  $Eu^d$  values of  $<30\%$  (Table GS-9-1). This deviation is interpreted to reflect positive  $Eu^d$  anomalies in the mafic source rocks for this greywacke. The REE contents of the chert sample (sample 7) are below detection limits (Figure GS-9-8b). Four of the sulphide-bearing samples show less LREE fractionation than the intermediate to mafic hostrocks. This indicates that these rocks have a different provenance than the hostrocks to the south of the mineralization and are not replacement sulphide bodies. The sulphidic sedimentary rock that occurs south of the chert layer is enriched in LREE relative to the

**Table GS-9-1: Selected trace-element analyses for rock samples from occurrence 10, south shore of Sheila Lake. All values in ppm. Negative values equal 'not detected' at that lower limit. Complete analytical dataset available in Data Repository item 2004005.**

Sample no.	Co	Ni	Cu	Zn	As	Zr	Nb	Mo	Ag	Sn	Sb	Hf	Ta	Pb	Bi	Th	U
42-10-01	14	-20	67	128	-5	89	3	2	-0.5	1	0.7	2.6	0.1	10	-0.4	1.5	1.3
42-10-01 (duplicate)	15	-20	60	127	-5	100	4	-2	-0.5	1	-0.5	3.1	0.1	11	-0.4	1.5	1.3
42-10-02	14	-20	16	108	-5	48	3	-2	-0.5	-1	-0.5	1.5	-0.1	8	-0.4	0.7	0.4
42-10-03	8	-20	91	126	67	102	6	-2	0.6	2	-0.5	3.0	0.4	8	-0.4	1.4	1.3
42-10-04	19	-20	111	118	11	78	5	-2	-0.5	1	-0.5	2.2	0.3	-5	-0.4	1.3	1.1
42-10-05	6	-20	79	110	-5	113	7	-2	-0.5	1	-0.5	3.3	0.4	8	-0.4	1.5	1.2
42-10-06	11	57	143	606	8	168	12	9	0.9	3	0.5	4.7	0.8	24	-0.4	2.5	4.9
42-10-06 (repeat)	12	45	100	627	6	174	13	8	0.6	4	1.3	4.7	0.8	25	0.5	2.5	4.8
42-10-07	-1	-20	19	-30	10	6	-1	-2	-0.5	-1	-0.5	-0.2	-0.1	-5	-0.4	-0.1	-0.1
42-10-08	10	26	119	152	-5	53	4	3	0.5	-1	-0.5	1.7	0.2	16	-0.4	0.4	0.7
42-10-09	11	28	113	111	76	69	5	3	0.5	2	-0.5	2.1	0.2	14	-0.4	0.7	0.8
42-10-10	8	108	463	530	-5	156	9	2	1.8	6	2.6	4.5	0.6	121	-0.4	2.2	2.6
42-10-11	94	468	1190	3060	896	26	2	16	3.6	2	5.8	0.8	0.1	92	4.0	0.5	5.6
42-10-12	12	42	161	301	19	74	6	5	1.0	-1	0.7	2.4	0.2	14	-0.4	1.1	1.6
42-10-13	7	47	130	338	35	85	6	3	0.7	-1	-0.5	2.7	0.2	20	-0.4	1.0	1.4
42-10-14	9	40	191	382	190	113	7	5	0.9	1	0.6	3.4	0.6	23	-0.4	1.5	2.5
42-10-15	11	67	148	322	33	142	9	4	1.0	1	0.9	4.4	0.4	30	-0.4	1.4	2.1
Rhyolite standard	-1	-20	12	208	12	71	6	-2	0.5	-1	1.0	2.2	0.1	31	-0.4	3.0	1.7

Sample no.	Eu <sup>d</sup>	La	Ce	Pr	Nd	Sm	Eu	Gd	Tb	Dy	Ho	Er	Tm	Yb	Lu
42-10-01	-8	9.5	22.4	2.73	13.4	3.7	1.14	3.9	0.8	4.7	1.1	3.3	0.53	3.4	0.54
42-10-01	-10	9.0	21.2	2.57	13.2	3.6	1.09	3.8	0.8	4.7	1.0	3.3	0.52	3.4	0.54
42-10-02	23	8.0	16.8	2.05	10.2	2.9	1.21	3.2	0.6	3.7	0.8	2.6	0.39	2.4	0.38
42-10-03	16	9.7	22.7	2.72	12.3	3.0	1.14	3.0	0.6	3.5	0.7	2.1	0.32	1.9	0.29
42-10-04	20	7.9	16.4	1.84	8.6	2.3	0.94	2.4	0.5	2.9	0.6	2.0	0.30	1.9	0.32
42-10-05	5	12.8	28.0	3.13	13.9	3.4	1.17	3.4	0.7	4.0	0.9	2.5	0.39	2.3	0.37
42-10-06	-7	15.3	35.3	4.03	17.9	4.5	1.38	4.5	0.9	5.2	1.1	3.2	0.48	2.9	0.47
42-10-07		0.5	1.1	0.10	0.6	0.2	-0.05	0.2	-0.1	0.2	-0.1	0.2	-0.05	0.2	-0.04
42-10-08	30	6.1	17.1	1.75	10.2	3.0	1.39	3.5	0.6	3.5	0.7	2.1	0.29	1.7	0.27
42-10-09	32	6.4	17.6	1.76	9.8	2.9	1.32	3.3	0.6	3.1	0.6	1.9	0.27	1.6	0.26
42-10-10	-14	11.0	27.3	2.53	13.3	4.0	1.23	4.9	0.9	5.6	1.2	3.8	0.56	3.5	0.56
42-10-11	-17	2.7	6.7	0.96	4.7	1.4	0.39	1.5	0.3	1.7	0.4	1.2	0.20	1.3	0.23
42-10-12	16	6.7	18.0	1.78	10.0	3.0	1.21	3.5	0.6	3.7	0.8	2.3	0.31	1.8	0.29
42-10-13	-4	8.6	23.9	2.38	13.8	4.0	1.36	4.7	0.8	4.7	1.0	3.1	0.44	2.8	0.44
42-10-14	-4	9.6	23.9	2.24	12.5	3.7	1.24	4.3	0.8	4.6	1.0	3.0	0.43	2.6	0.42
42-10-15	-20	11.7	31.6	3.15	17.3	5.3	1.44	5.8	0.9	5.5	1.2	3.5	0.50	3.1	0.49
Rhyolite standard	-20	15.1	33.2	3.13	14.6	3.1	0.80	2.9	0.5	2.7	0.6	1.8	0.26	1.6	0.26

other sulphide-bearing rocks, and has Eu<sup>d</sup> values near zero. Samples 8 and 9, with 5 and 20% pyrite, respectively, occur immediately north of sample 7. These two samples have a flat LREE pattern that differs from both the hostrocks and the sulphidic sedimentary rock south of the chert. Sample 12, with only trace pyrite, has LREE and HREE patterns identical to those of samples 8 and 9. All three samples have positive Eu<sup>d</sup> values. Similar positive Eu<sup>d</sup> patterns have been observed in ores and distal exhalite in and around massive sulphide deposits (Gale et al., 1997, 1999; Gale, 2003).

Samples 10 and 15 (Figure GS-9-8a), each with <10% pyrite, exhibit a stronger LREE enrichment relative to other

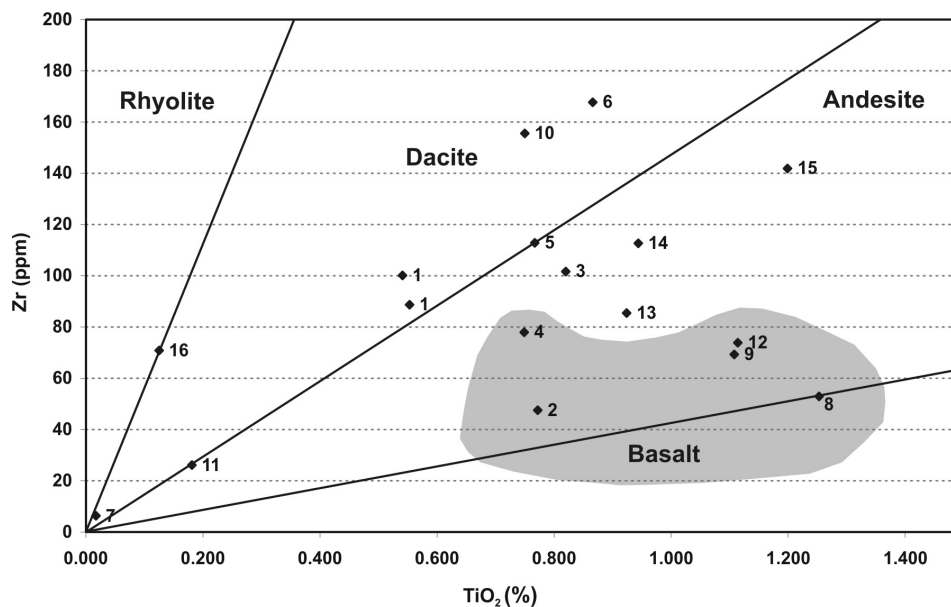


**Figure GS-9-3:** Plot of  $TiO_2$  versus Zr in rock samples from occurrence 10. On this diagram, the rhyolite standard (sample 16) plots in the field normally occupied by rhyolite, basalt normally plots in the vicinity of the lower line, and andesite normally plots in the vicinity of the line that passes through samples 11 and 5 (Gale and Dabek, 1996).

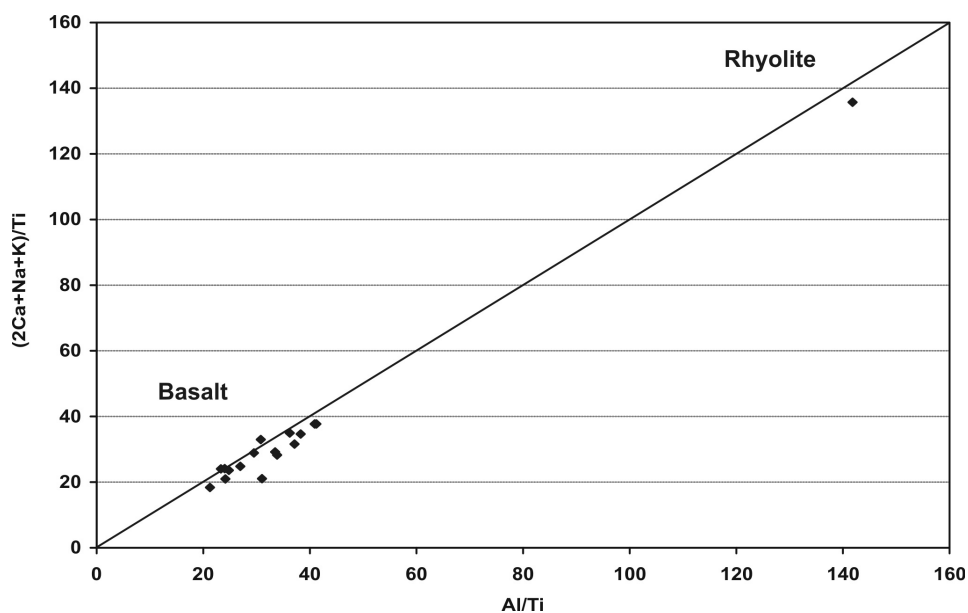


**Figure GS-9-4:** Plot of molar ratios of alkali elements and  $TiO_2$  for rock samples from occurrence 10. The rhyolite standard plots at the right of the diagram and indicates that these sedimentary tuffaceous rocks do not have a significant felsic volcanic component (cf. Madeisky, 1995).

sulphide-bearing rocks, but less than the hostrocks. These rocks have low negative  $Eu^d$  values. Sample 11, with approximately 50% pyrrhotite, has a REE pattern that is similar to the pyritic rocks, and a positive  $Eu^d$  value. The reason for the absence of a positive  $Eu^d$  in sample 11 is uncertain; it may reflect sulphide deposition from a low-temperature fluid or formation of pyrrhotite by mobilization during postdepositional structural and metamorphic events.

Samples 10 and 11 have higher Ni, Cu, Zn, Ag, Sb and Pb concentrations than the hostrocks; As, Bi and Mo are also higher in sample 11 (Table GS-9-1). These are common pathfinder elements in exhalites related to volcanogenic massive sulphide deposits. Samples 8, 9 and 12, with positive  $Eu^d$  values, are not anomalous in any of the pathfinder elements. The presence of anomalous pathfinder elements and  $Eu^d$  in different strata may reflect different pulses of hydrothermal activity from a vent.

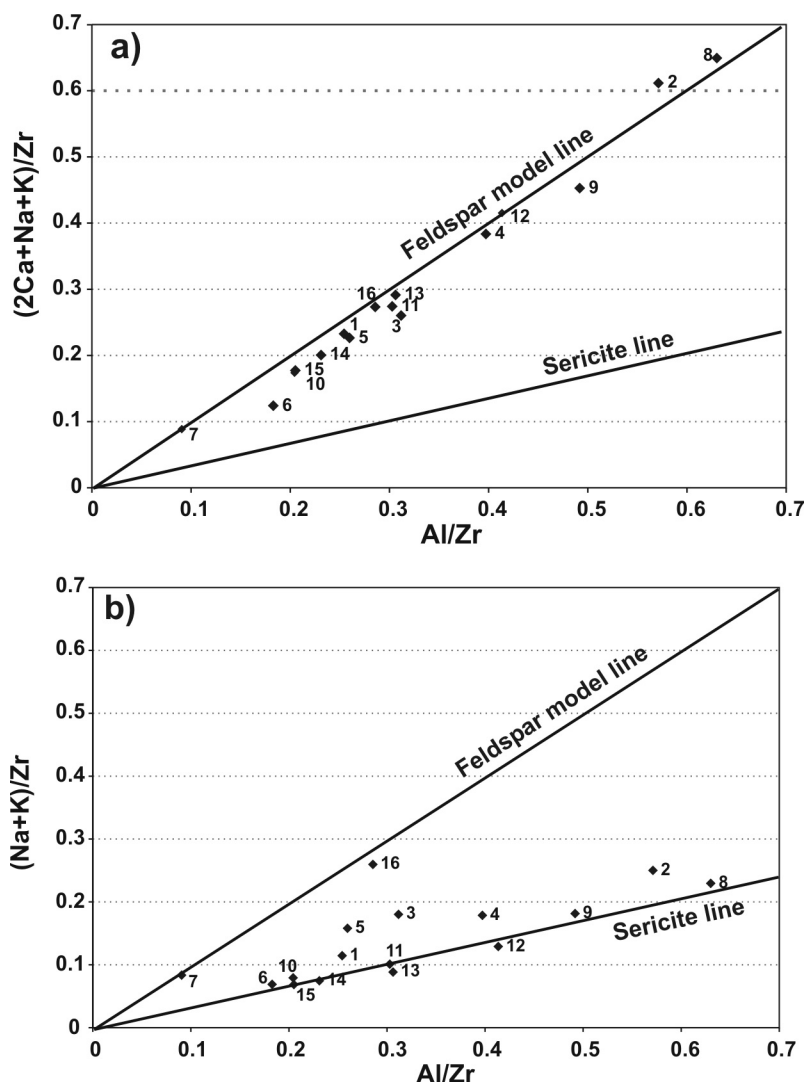


**Figure GS-9-5:** Plots of molar ratios for rock samples from occurrence 10: **a)** of alkali elements, Al and Zr (after Madeisky, 1995). On this diagram, unaltered felsic rocks plot along the feldspar model line and unaltered mafic volcanic rocks plot above the line. Altered rocks plot below the feldspar model line and toward the sericite line (slope = 1/3). **b)** of alkali elements (minus Ca), Al and Zr. The samples plot farther away from the feldspar model line (slope = 1) than in Figure GS-9-5a; this indicates that calcic plagioclase, rather than calcite, is a component of these rocks and there is minimal Ca metasomatism.

### **Spruce bark**

Selected data for samples of spruce bark, collected at 25 m intervals across the sulphide-bearing zone, are presented in Table GS-9-2. Complete analytical results are included in Data Repository item 2004005. Anomalous values are shown graphically in Figures GS-9-9 to -13. Samples 2B and 3B are located approximately over the sulphide-bearing zone with anomalous metal concentrations (Figure GS-9-2). Zinc concentrations (Table GS-9-2) are higher in the two bark samples overlying the zone. However, the contrast in Zn concentrations is not as strong as those for Cu (Figure GS-9-9), Mo, Ag and Sb (Figure GS-9-10), and Pb (Figure GS-9-12). Europium and dysprosium (Figure GS-9-13), and the other REE, are enriched in the bark of spruce trees that grow over the mineralized zone. All of the samples have negative  $\text{Eu}^d$  values.

Rock samples from the mineralized zone are not enriched in the REE and several have lower REE values with respect to the surrounding hostrocks. Therefore, increased REE values in the bedrock cannot account for the anomalous REE contents in the ashed spruce bark. The increased REE contents in bark can be interpreted to be a result of an electrochemical cell associated with the sulphide mineralization. It is postulated that oxidation of the sulphides during

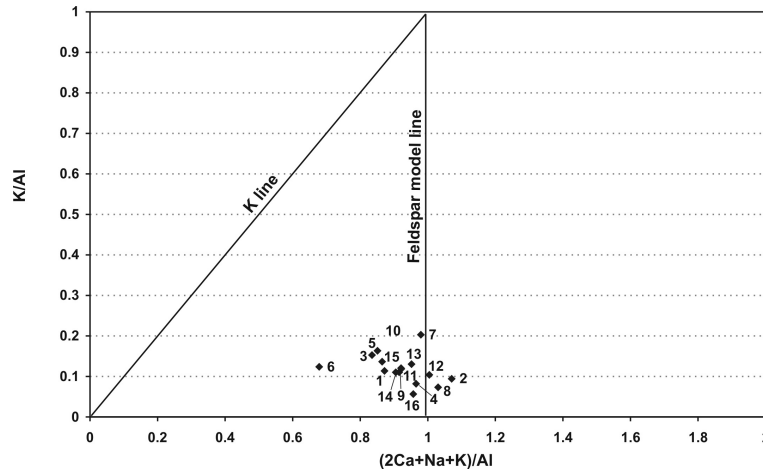


**Figure GS-9-6:** Molar-ratio plot to illustrate K metasomatism (after Madeisky, 1995) for rock samples from occurrence 10. Unaltered rocks plot to the right of the feldspar model line. Rocks that have undergone K metasomatism plot to the left of the feldspar model line; if all Na and Ca are replaced by K, the samples will plot on the K Line. Calcium addition causes the samples to plot to the right of the feldspar model line, whereas both alkali depletion and K addition cause samples to plot to the left of this line.

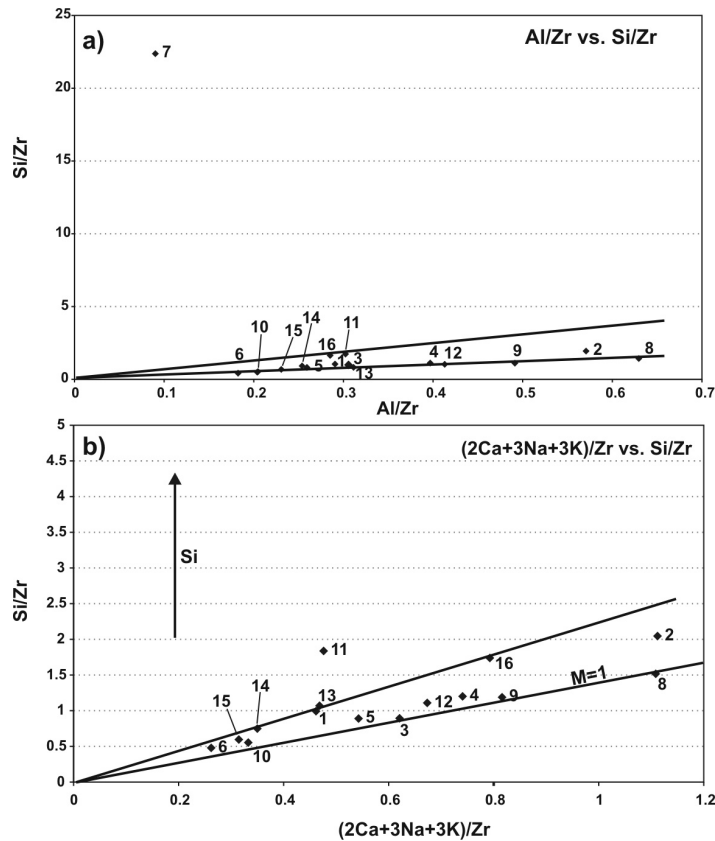


**Figure GS-9-7:** Molar-ratio plots for rock samples from occurrence 10: **a)** to illustrate silicification (after Madeisky, 1995). Only sample 7 has abundant free quartz and plots well away from the trend of the intermediate to mafic rocks (i.e., the Si content is independent of Al-bearing minerals). Most of the samples plot between the two lines on the diagram and show that there is little variation in their composition. **b)** to show relative silica metasomatism when modelled against feldspar, pyroxene, biotite and sericite, which should plot on the model line with slope ( $m$ ) = 1. Calcium addition would cause the samples to plot below the line with  $m = 1$ , the conclusion being that there is little Ca metasomatism in these rocks. The diagram does not distinguish between Si addition and alkali metasomatism. Only sample 7, which plots above the diagram, and sample 11 show evidence of possible Si addition.

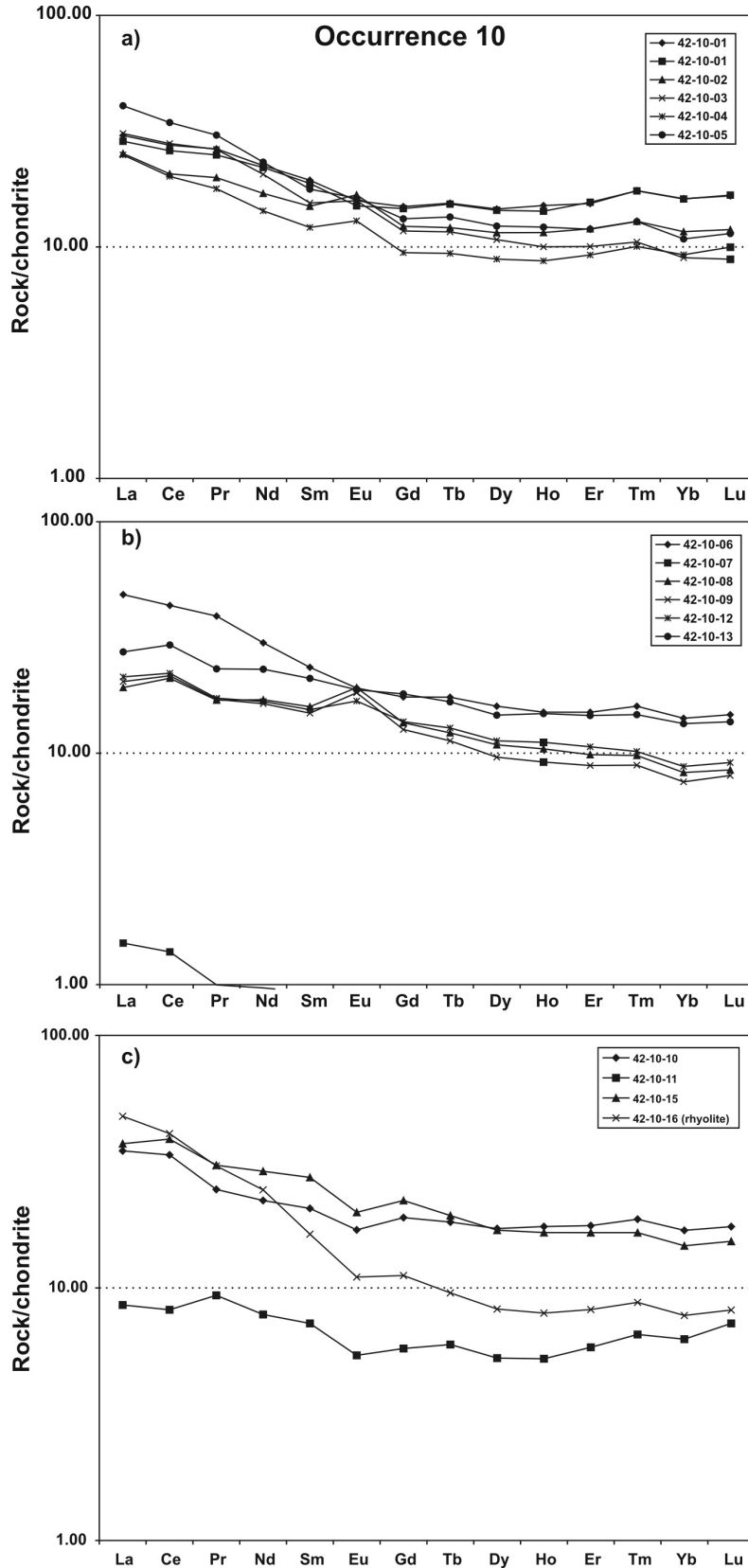


**Figure GS-9-8:** Rare earth element plots for rock samples from occurrence 10: **a)** sulphide-free hostrocks; **b)** sulphide-bearing rocks with near-zero and positive  $Eu^d$  values; **c)** three sulphide layers and rhyolite standard.

**Table GS-9-2: Selected analyses for ashed spruce bark, occurrence 10, south shore of Sheila Lake.  
Complete analytical dataset available in Data Repository item 2004005.**

Sample no.	Co	Ni	Cu	Zn	Y	Mo	Ag	Cd	Sb	Eu	Dy	Er	Tl	Pb	Bi	Th	U
42-10-1B	20.0	536	971	3,820	1.94	0.8	1.8	7.68	0.49	0.111	0.343	0.181	0.640	82.9	0.21	0.561	0.519
42-10-2B	39.8	1190	1830	4100	3.36	1.4	1.9	11.0	1.00	0.180	0.606	0.329	1.13	178	0.53	0.659	0.706
42-10-3B	33.3	1180	2430	4180	3.54	1.6	2.5	12.7	1.18	0.203	0.657	0.351	2.36	197	0.82	0.753	0.699
42-10-4B	43.5	1160	1310	3180	1.47	0.8	1.7	7.55	0.51	0.079	0.268	0.143	0.210	71.9	0.18	0.496	0.229
42-10-5B	15.2	496	1440	2750	2.31	0.9	1.7	6.79	0.55	0.130	0.399	0.206	0.288	98.9	0.45	0.535	0.331

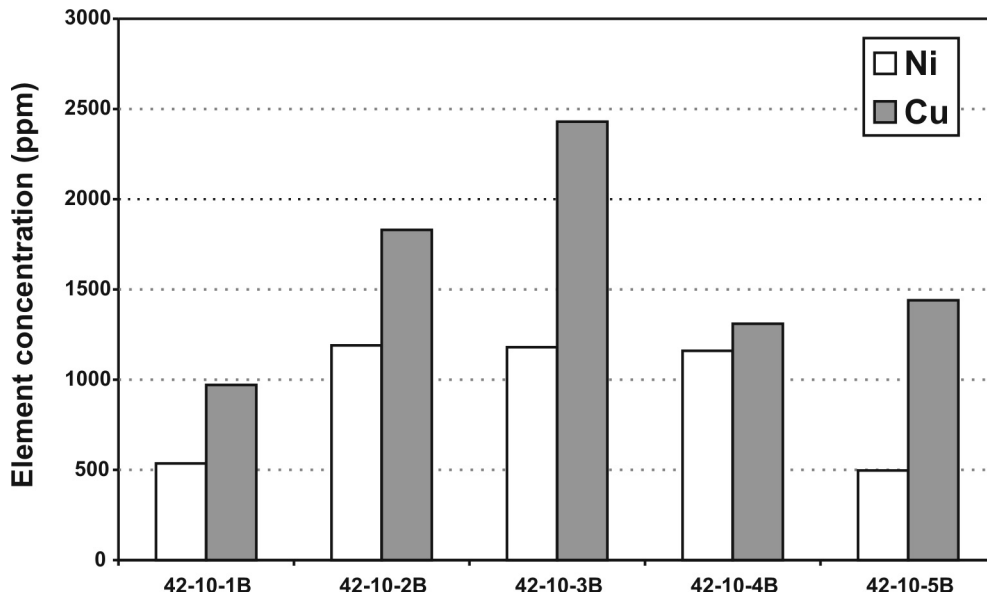


**Figure GS-9-9: Distribution of Ni and Cu concentrations in the ashed outer bark of spruce trees, occurrence 10.**

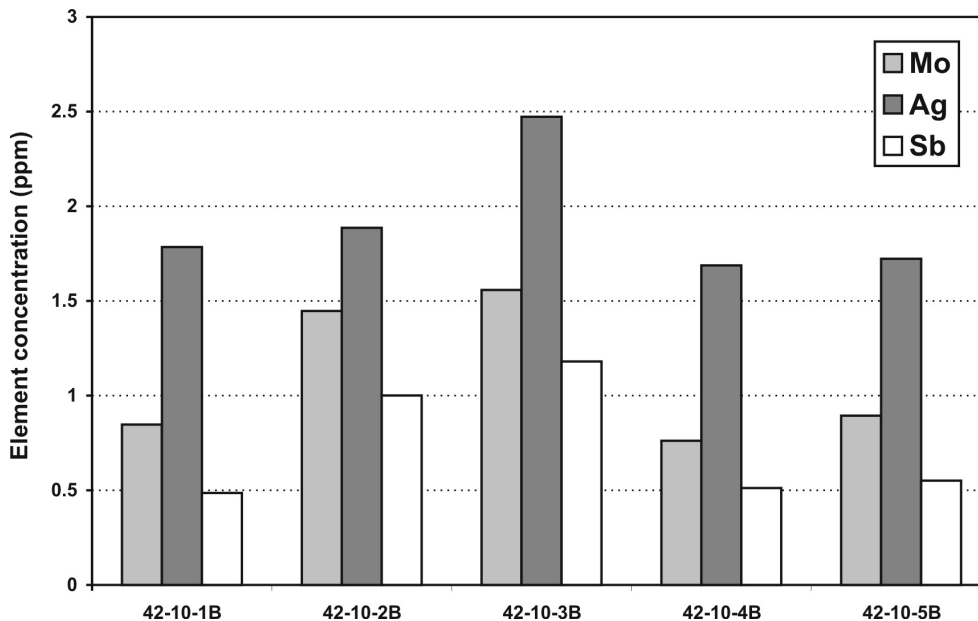


**Figure GS-9-10: Distribution of Mo, Ag and Sb concentrations in the ashed outer bark of spruce trees, occurrence 10.**

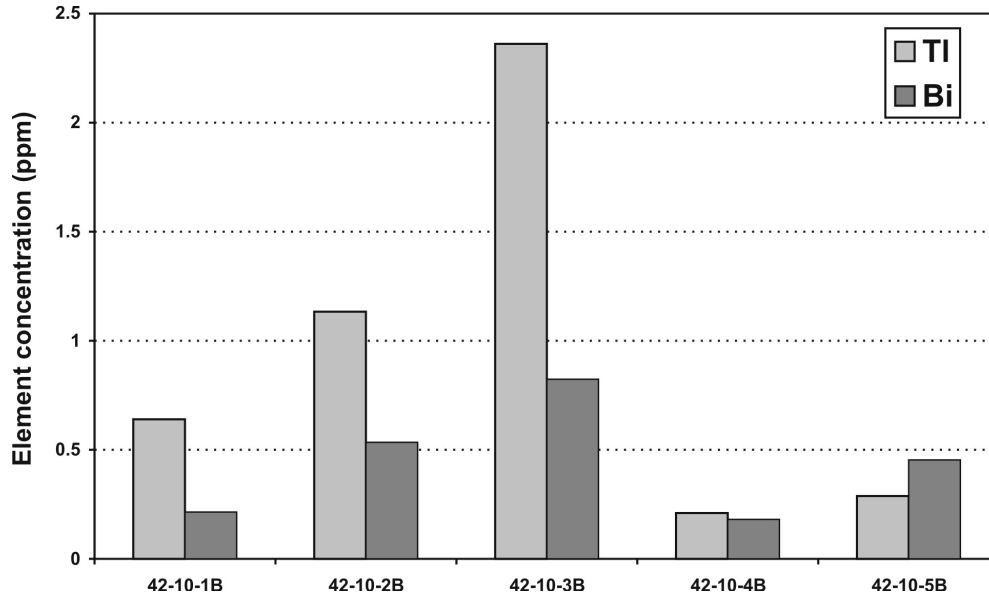


Figure GS-9-11: Distribution of Tl and Bi concentrations in the ashed outer bark of spruce trees, occurrence 10.

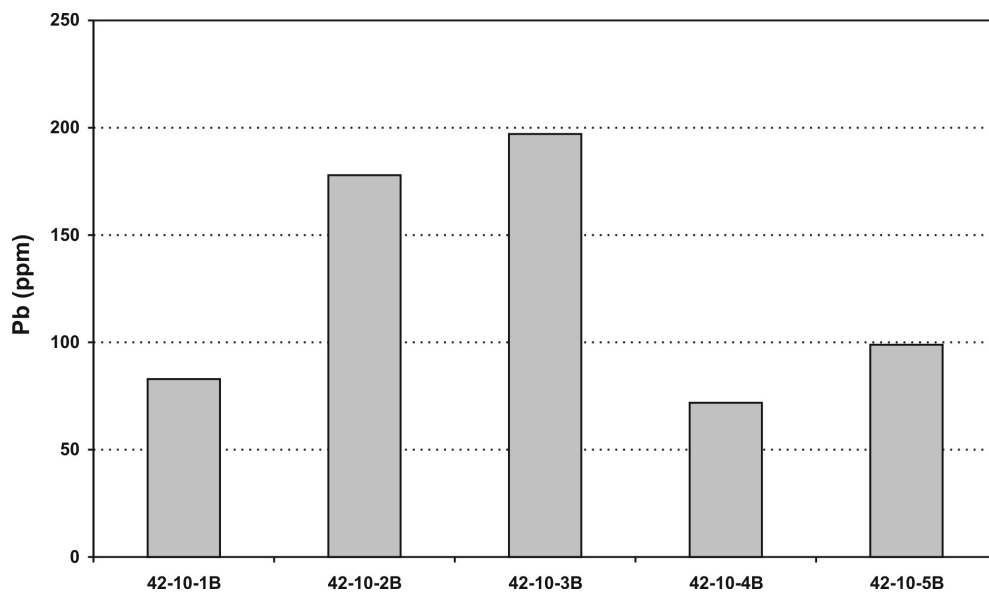


Figure GS-9-12: Distribution of Pb concentrations in the ashed outer bark of spruce trees, occurrence 10.

weathering released base and precious metals that were then transported to the near-surface root systems of the spruce trees. It should be noted that the depth of soil covering bedrock at this location is commonly less than 30 cm. Therefore, it cannot be assumed that similar results will be observed in areas with thick overburden.

### Economic considerations

The sulphide strata exposed on Sheila Lake are interpreted to be a distal exhalite and have the potential to be associated with a massive sulphide deposit. Spruce bark over the mineralized zone is anomalous in a number of elements, including total REE, and appears to be a viable exploration medium in areas of shallow overburden.

### Acknowledgments

Paul Pawliw of Black Hawk Mining Inc. is thanked for providing copies of geological and geophysical maps and drill logs, and for assistance in the location of and access to drillcore.

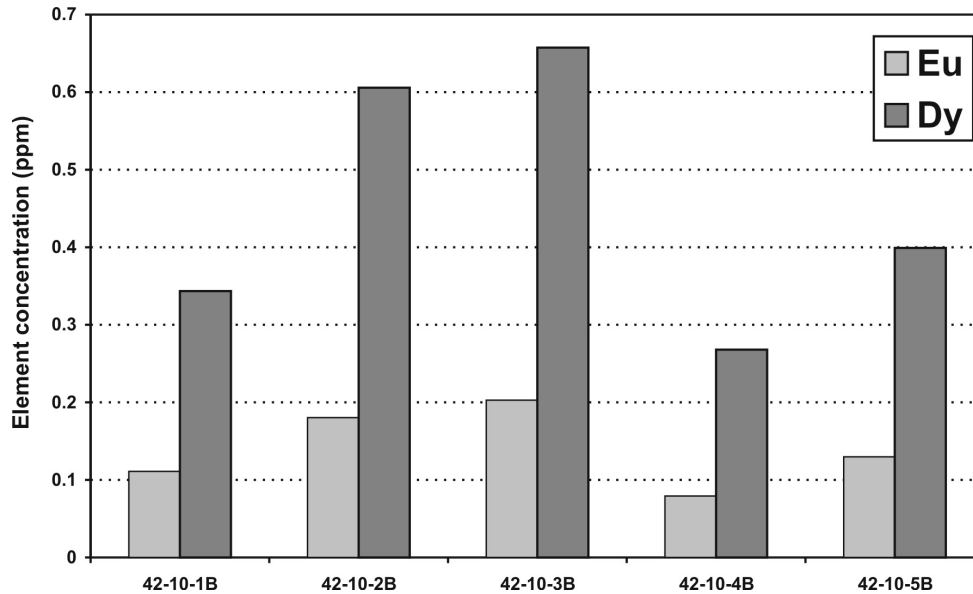


**Figure GS-9-13:** Distribution of Eu and Dy concentrations in the ashed outer bark of spruce trees, occurrence 10.

## References

- Baldwin, D.A. 1989: Mineral deposits and occurrences in the Lynn Lake area, NTS 64C/14; Manitoba Energy and Mines, Geological Services, Mineral Deposits Series, Report 6, 130 p.
- Gale, G.H. 2003: Vectoring volcanogenic massive sulphide deposits using rare earth elements and other pathfinder elements at the Ruttan mine, Manitoba (NTS 63B5); *in* Report of Activities 2003, Manitoba Industry, Economic Development and Mines, Manitoba Geological Survey, p. 54–73.
- Gale, G.H. and Dabek, L.B. 1996: The Baker Patton Complex (parts of 63K/12 and 63K/13) – rhyolites, dacites and rare earth element chemistry; *in* Report of Activities 1996, Manitoba Energy and Mines, Geological Services, p. 47–51.
- Gale, G.H., Dabek, L.B. and Fedikow, M.A.F. 1997: The use of rare earth element analyses in the exploration for massive sulphide type deposits in volcanic rocks – progress report; *in* Report of Activities 1997, Manitoba Energy and Mines, Geological Services, p. 147–55.
- Gale, G.H., Dabek, L.B. and Fedikow, M.A.F. 1999: The application of rare earth element analyses in the exploration for volcanogenic massive sulphide type deposits; *Exploration and Mining Geology*, v. 6, no. 3, p. 233–252.
- Madeisky, H.E. 1995: Quantitative analysis of hydrothermal alteration: applications in lithogeochemical exploration; unpublished report, HEMAC Exploration Ltd., P.O. Box 848, Station A, Vancouver BC, Canada V6C 2N7, 233 p.